Journal of High School Science

Selective KRAS dependency in cancer: Therapeutic implications for KRAS-mutant tumors

Mai B.J

Submitted: April 25, 2025, Revised: version 1, June 25, 2025
Accepted: June 27, 2025

Abstract
KRAS is a well-established oncogene and a key driver of various cancers, particularly pancreatic, colorectal, and lung cancers. This study explored the selective dependency of cancer cells on KRAS, highlighting its potential as a therapeutic target. DepMap analysis revealed that KRAS dependency was highly tumor-type specific, with significant reliance observed in cancer cell lines harboring KRAS mutations. Both CRISPR knockout and RNAi screens consistently demonstrated that KRAS-mutant cancer cells were critically dependent on KRAS for survival. In pancreatic cancer cell lines, KRAS knockout resulted in a pronounced reduction in cell viability, underscoring its role as a vital driver of cancer cell proliferation. Immunohistochemical analysis further revealed variable KRAS protein expression across cancer types, suggesting context-dependent KRAS dysregulation in tumorigenesis. These findings highlight KRAS as a critical and selective vulnerability in pancreatic and other KRAS-driven cancers, emphasizing the need for personalized therapeutic strategies. As KRAS inhibitors continue to advance in clinical development, they hold promise for significantly improving outcomes in patients with KRAS-driven malignancies.

Keywords
KRAS, Pancreatic cancer, Kirsten RAt Sarcoma virus, Tumorigenesis, CRISPR, RNAi, Oncogene, sgRNA, DepMap, Immunoassay

Benjamin J Mai, Carlmont High School, 1400 Alameda de las Pulgas, Belmont, CA 94002, USA.
Benjaminmai2008@gmail.com

https://doi.org/10.64336/001c.141477

Introduction

The Dependency Map (DepMap) (1) (https://depmap.org/portal) is a vital tool in cancer research, helping identify therapeutic targets by analyzing data from diverse cancer cell lines to pinpoint genes critical for cancer cell survival and growth. By integrating screening data with genetic information, DepMap reveals genes that, when inhibited, can selectively kill cancer cells while sparing normal ones, making it invaluable for developing targeted cancer treatments. Additionally, DepMap provides tools like CRISPR and RNA interference to experimentally validate these targets, ensuring their importance before advancing to preclinical studies. By focusing on well-validated targets such as KRAS in pancreatic cancer, DepMap accelerates drug discovery, paving the way for more effective, personalized therapies.

The KRAS gene produces a protein that is vital for controlling cell growth, division, and survival via the RAS/MAPK signaling pathway (2). KRAS is one of the most commonly mutated oncogenes in cancers such as lung, colorectal, and especially pancreatic cancer, which is notably aggressive and difficult to treat (3). In pancreatic cancer, KRAS mutations are present in about 85% of tumors, making it a key driver of the disease (4). These mutations disrupt normal cellular signaling, creating conditions that promote tumor growth, immune evasion, and resistance to apoptosis (programmed cell death) (5).

The prevalence and impact of KRAS mutations have made them a central focus in cancer research, with scientists actively exploring ways to directly target KRAS or interfere with its downstream signaling pathways (6). Small molecule inhibitors, in particular, represent a significant advance in cancer treatment by specifically targeting proteins or pathways essential for tumor growth and survival. This targeted approach enhances treatment effectiveness while reducing side effects compared to traditional chemotherapy (7). The development of these inhibitors involves multiple steps, starting with the identification and validation of targets using techniques such as genomics. Researchers then screen chemical libraries to find compounds that interact with these targets, refining them to improve efficacy and minimize toxicity. Advances in structural biology, such as X-ray crystallography and NMR spectroscopy, along with computer modeling, have significantly aided this process by providing detailed views of protein structures and simulating drug-target interactions (8).

As drug discovery methods evolve, small molecule inhibitors remain vital in developing more effective cancer therapies, especially for those driven by KRAS mutations. In this study, KRAS was analyzed as a cancer target using DepMap and other databases. CRISPR knockout experiments were performed to measure the impact of KRAS on cell growth in various cell lines. The methods employed in this research can be further expanded for the identification and validation of novel targets in cancer drug discovery.

Materials and Methods

Thawing of cells

Frozen cell vials were retrieved from liquid nitrogen storage and rapidly thawed in a 37°C water bath for 1-2 minutes until only a small ice pellet remained. Once completely thawed, the vial was disinfected with 70% ethanol before opening it in a sterile flow hood. The contents of the vial were transferred to a 15 mL conical tube containing 9 mL of pre-warmed complete growth medium. The cell suspension was centrifuged at 200 x g for 5 minutes to pellet the cells. The supernatant containing dimethyl sulfoxide (DMSO) was carefully aspirated, and the cell pellet was resuspended in fresh, pre-warmed medium. The resuspended cells were then transferred to a flask and incubated at 37°C in a humidified atmosphere of 5% CO_2. Cell viability and cell number were analyzed by cell counter Vi-CELL BLU (Beckman Coulter).

Cell culture

AsPC1 (CRL-1682, ATCC, Manassas, VA, USA), T3M4 (Cat#CSC-C6425J, Creative Bioscience, Salt Lake City, UT, USA), and BxPC3 (CRL-1687, ATCC) cells used in this study were cultured in RPMI-1640 medium (Cat# 11875093, Gibco, Thermo Fisher Scientific, Waltham, MA, USA) supplemented with 10% fetal bovine serum (FBS) (Cat# A5670701, Gibco, Thermo Fisher Scientific) and 1% penicillin-streptomycin (Cat# 10378016, Gibco, Thermo Fisher Scientific). Panc 04.03 cells (CRL-2555, ATCC) were cultured in RPMI-1640 medium supplemented with 10% FBS, 1% penicillin-streptomycin, and 10 µg/ml insulin (Cat# 12585014, Gibco, Thermo Fisher Scientific). Capan-1 cells (HTB-79, ATCC) were cultured in Iscove's Modified Dulbecco's Medium (IMDM) (Cat# 12440053, Gibco, Thermo Fisher Scientific) supplemented with 20% FBS and 1% penicillin-streptomycin. PANC-1 cells (CRL-1469, ATCC) were cultured in Dulbecco's Modified Eagle Medium (DMEM) (Cat# 11965118, Gibco, Thermo Fisher Scientific) supplemented with 10% FBS and 1% penicillin-streptomycin. MIA PaCa-2 cells (Cat#85062806, Sigma Aldrich, St. Louis, MO, USA) were cultured in DMEM supplemented with 10% FBS, 1% penicillin-streptomycin, and 2.5% horse serum (Cat#16050130, Gibco, Thermo Fisher Scientific). The cultures were maintained at 37°C in a humidified incubator with a 5% CO_2 atmosphere. The medium was replaced every 2-3 days, and the cells were sub-cultured when they reached approximately 70-80% confluency. For passage, cells were detached using 0.25% trypsin-EDTA (Cat# 25200056, Gibco, Thermo Fisher Scientific) after washing with Dulbecco's phosphate-buffered saline (DPBS) (Cat# 14190144, Gibco, Thermo Fisher Scientific) and reseeded at appropriate densities (9).

Cell morphology imaging

Cell imaging was performed using the EVOS M5000 Imaging System (Thermo Fisher Scientific), and cells were cultured in flasks for imaging. For brightfield imaging, cells were imaged at magnification 20X using the phase-contrast objective. Image acquisition was performed using the system's built-in software, allowing for real-time observation and high-

resolution image capture. The software's automated functions, such as autofocus and exposure control, were utilized to optimize image quality. Images were saved in TIFF format for further analysis (10).

Protein detection

Protein detection was performed using the Jess system (Cat# 004-650, ProteinSimple, San Jose, CA, USA) following the manufacturer's guidelines (11). Cell lysates were prepared using RIPA buffer (Cat# 89900, Thermo Fisher Scientific) supplemented with protease inhibitors (Cat# 78429, Thermo Fisher Scientific), with cells lysed on ice for 30 minutes and centrifuged at 14,000 × g for 10 minutes at 4°C. Samples were diluted in Jess sample buffer and denatured by heating at 95°C for 5 minutes, with final concentrations adjusted to 0.5–1.0 µg/µL. The Jess system was loaded with 5 µL of each sample, and proteins were separated by capillary electrophoresis, followed by immobilization within the capillaries. Immunodetection was performed by incubating proteins with primary antibodies specific to the target proteins, PLK1 (Cat# 4535, Cell Signaling Technology, Danvers, MA, USA), KRAS (Cat# 415700, Invitrogen, Carlsbad, CA, USA), GAPDH (Cat# 9545, Sigma Aldrich), followed by HRP-conjugated secondary antibodies, Anti-Mouse Secondary HRP (Cat# 042-205, ProteinSimple) and Anti-Rabbit Secondary HRP (Cat# 042-206, ProteinSimple). After washing with Jess wash buffer, chemiluminescent detection was performed using a substrate for HRP. The resulting signals were captured and quantified using the ProteinSimple Compass software following the user manual (Compass for SW Version 7.0).

Cell viability assay

Cell viability was assessed using the CellTiter-Glo® Luminescent Cell Viability Assay according to the manufacturer's protocol. Briefly, cells were seeded in white-walled 96-well plates (Cat# 3903, Corning, Corning, NY, USA) at a density of 1250 cells per well and allowed to grow for 5 days. 100 µL of CellTiter-Glo® reagent (Cat# G9241, Promega, Madison, WI, USA) was added to each well, followed by gentle shaking for 2 minutes to induce cell lysis. The plate was incubated at room temperature for 10 minutes to stabilize the luminescent signal. Luminescence, which is proportional to the amount of ATP present and thus an indicator of metabolically active cells, was measured using PherastarFSX multi-mode plate reader (BMG Labtech, Cary, NC, USA) equipped with Luminescence Detection Module, using the following settings: integration time of 1.0 second, gain set to 3000, and top-read mode following the manufacturer's setting. All measurements were performed at room temperature in triplicate. Luminescence data were recorded as relative luminescence units (RLUs) and normalized to control sgRNA- or DMSO-treated samples, as previously described (12). Data were analyzed using GraphPad Prism (version 10.0), and results are presented as mean ± standard deviation.

Gene editing by CRISPR

CRISPR-mediated gene editing was performed using the ribonucleoprotein (RNP) approach

with gRNAs and Cas9 (SpCas9 2NLS Nuclease, Synthego, Redwood City, CA, USA) from Synthego. Synthetic single guide RNAs (sgRNAs) targeting KRAS, PLK1 or control sgRNAs (Gene Knockout Kit, Synthego) were designed using Synthego's CRISPR design tool and purchased pre-assembled. The sgRNAs were complexed with recombinant Cas9 protein at a ratio of 3:1 to form RNP complexes. The cells were electroporated with the RNP complexes using the Neon Transfection System (Cat# MPK5000, Thermo Fisher Scientific). Specifically, 100,000 cells were resuspended in Neon R Buffer (Cat# MPK1025, Thermo Fisher Scientific) and mixed with the RNP complex. The mixture was electroporated (program 1750/20/1) according to the manufacturer's protocol (13). Immediately following electroporation, the entire cell population was transferred into pre-warmed complete medium and cultured for 5 days prior to performing the cell growth assay and protein detection. No cell selection was carried out after RNP electroporation.

Results

KRAS as a selective target for pancreatic cancer cells

From the DepMap analysis (Figure 1A), KRAS emerged as a highly selective target. Unlike commonly essential genes, such as PLK1, which show broad essentiality across various cancer types, KRAS demonstrates a more tumor-type-specific dependency. Specifically, KRAS dependency is not confined to pancreatic cancer alone but is also observed in colorectal and lung cancer cell lines (Figure 1B). These results align with the known biology of KRAS, as mutations in this oncogene are highly prevalent in these cancer types, further reinforcing the notion that KRAS is a context-dependent vulnerability in specific cancer settings. In addition to the CRISPR screen, RNA interference (RNAi) analysis (Figure 1C) further supports the selective role of KRAS in pancreatic and colorectal cancer cell lines, with minimal off-target effects in other cell types. The convergence of evidence underscores the potential of KRAS as a high-priority therapeutic target, particularly in pancreatic cancer, where alternative therapeutic options are limited.

KRAS dependency in cancer cell lines with KRAS mutations

To further dissect the role of KRAS in cancer cell growth, its dependency across a range of cancer cell lines harboring KRAS mutations was measured. Specifically, Figure 2A presents a scatter plot where each point corresponds to a different cancer cell line from lung, colorectal, or pancreatic origins. The position of these points, reflecting the KRAS gene effect, revealed that cell lines with KRAS mutations exhibited significantly lower KRAS knockout scores, indicating a heightened dependency on KRAS for survival. This suggests that cancer cells with mutated KRAS are particularly reliant on its continuous activity, reinforcing the idea that KRAS functions as a critical oncogene in these types of cancer. Figure 2B further validates this observation by demonstrating a strong correlation between KRAS dependency scores derived from two independent functional screening approaches:

CRISPR-based knockout and RNA interference (RNAi). This cross-method validation provided robust evidence that KRAS dependency is not an artifact of a single screening technique but a true biological phenomenon.

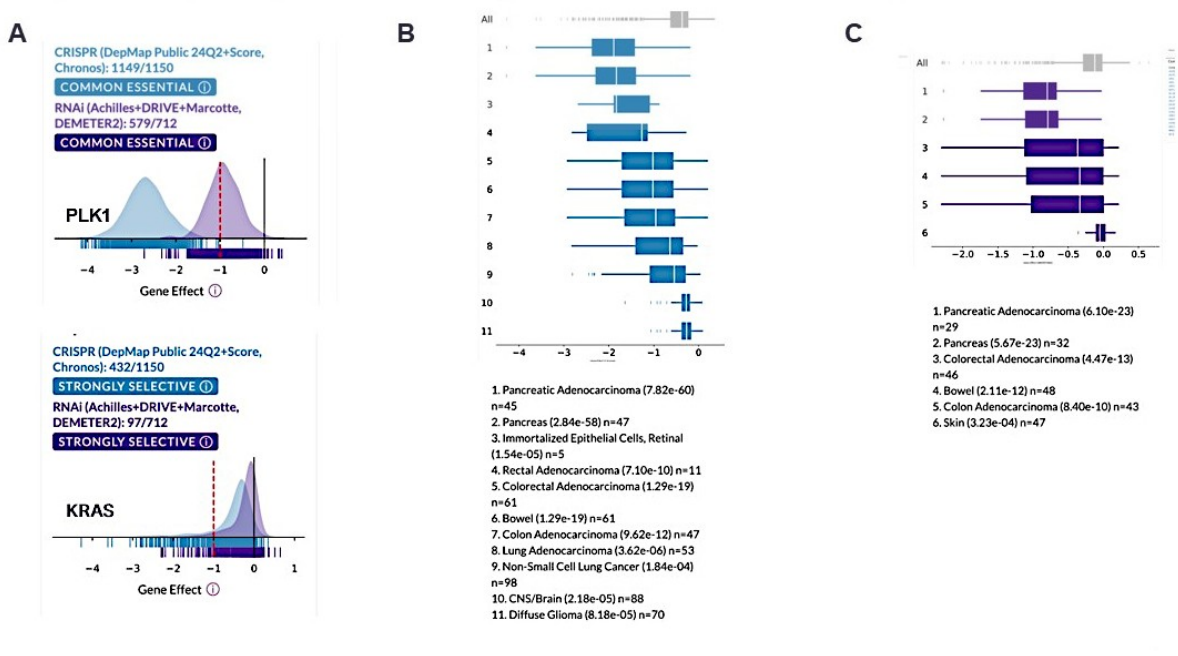

Figure 1. KRAS is a strongly selective target in pancreatic cancer cell lines. **A.** Distinction between strongly selective (KRAS) and common essential (PLK1) genes as identified in the DepMap CRISPR and RNAi screening dataset. **B.** Selective dependency of KRAS in pancreatic, colorectal and lung adenocarcinoma cells as identified in DepMap CRISPR screening dataset. **C.** Selective dependency of KRAS in pancreatic and colorectal adenocarcinoma cells as identified in DepMap RNAi screening dataset.

To validate the dependency of KRAS in more detail, a subset of seven pancreatic cancer cell lines, selected based on their KRAS mutation status and DepMap gene effect scores (Table 1) were selected for analysis. These cell lines were chosen to represent a spectrum of KRAS mutation profiles, allowing us to examine how variations in KRAS mutations influence cancer cell survival and therapeutic response. Table 1 provides a comprehensive overview of each cell line, detailing important characteristics such as their growth conditions, doubling times, and KRAS dependency scores (data from DepMap). Notably, all seven cell lines exhibit an adherent epithelial phenotype, yet display variability in their growth rates and KRAS mutations.

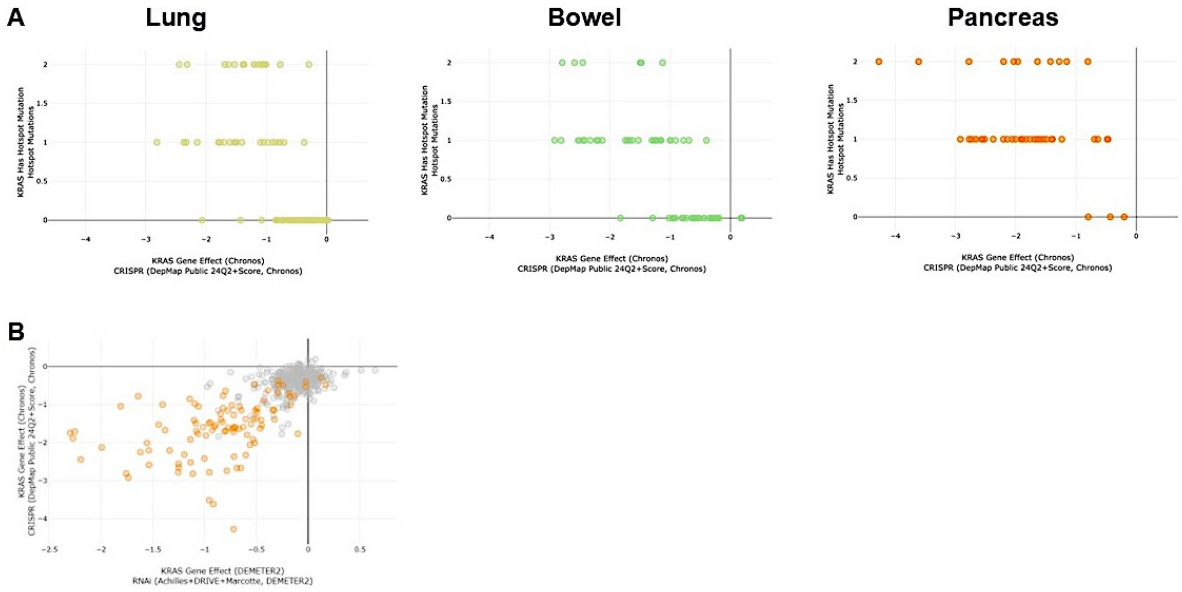

Figure 2. Analysis of KRAS dependency across cell lines with KRAS mutations from various cancer indications. **A.** Scatter plot showing KRAS dependency scores from CRISPR screen across a diverse set of cancer cell lines. Each point represents a single cell line, with the x-axis indicating the Gene effect with KRAS knockout and the y-axis representing the KRAS mutation status (0 indicates no mutations, 1 and 2 indicate mutations). Lower scores indicate higher dependency on KRAS for cell survival. **B.** Correlation of KRAS dependency from CRISPR and RNAi screening dataset. Each orange dot indicates one cell line with KRAS mutations (Pearson Correlation: 0.449, p-value: 2.44×10^{-6}).

Table 1. Characteristics of selected pancreatic cancer cell lines from KRAS dependency study.

Cell line	Culture medium	Doubling time (h)	KRAS Gene effect (Chronos)	KRAS mutations
AsPC-1	RPMI-1640 Medium – 10% FBS	58	-4.27	G12D
Panc 04 03	RPMI-1640 Medium – 10% FBS (+10 ug/mL Insulin)	50.5	-2.92	G12D
Capan-1	Iscove's Modified Dulbecco's Medium – 20% FBS	60-80	-1.97	G12V
PANC-1	Dulbecco's Modified Eagle's Medium – 10% FBS	52-56	-1.69	G12D
MIA PaCa-2	Dulbecco's Modified Eagle's Medium – 10% FBS and 2.5% Horse serum	26	-2.78	G12C
T3M4	RPMI-1640 Medium – 10% FBS	23	-0.69	Q61H
BxPC-3	RPMI-1640 Medium – 10% FBS	48-60	-0.47	Wild-type

This table provides detailed information on the selected cancer cell lines used in the KRAS dependency study. The data includes culture medium, doubling time, cellular morphology (Adherent epithelial), KRAS Gene Effect from DepMap CRISPR and specific KRAS mutations present in each cell line.

Morphological analysis of pancreatic cancer cell lines

A detailed morphological comparison of several pancreatic cancer cell lines is presented in Figure 3 to ensure the accuracy and validity of the *in vitro* models.

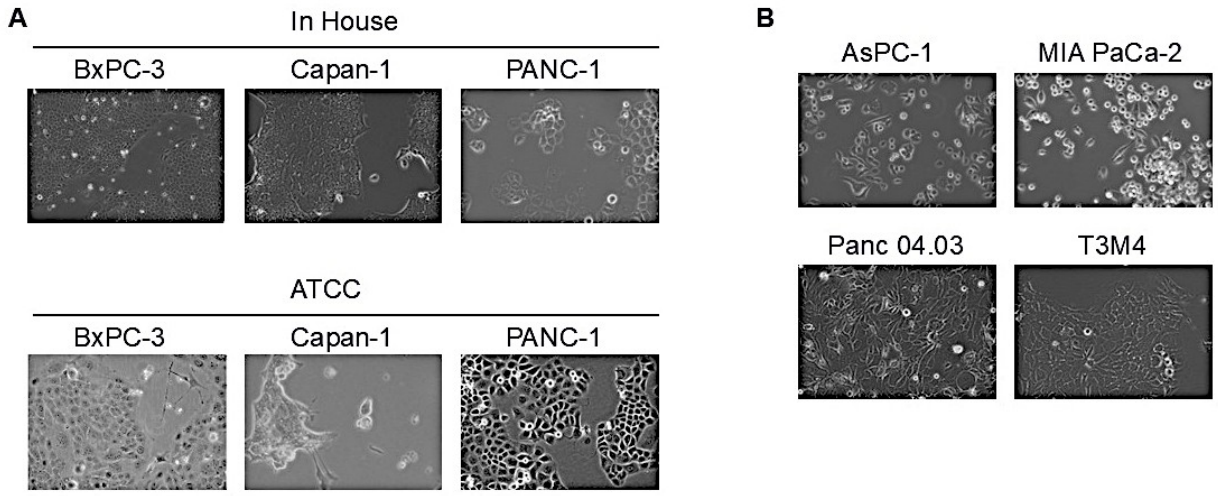

Figure 3. Morphological characteristics of selected cancer cell lines observed under microscopy (20X magnification). **A.** Pancreatic cancer cell lines BxPC-3, Capan-1 and PANC-1 contrasting images obtained from the ATCC website with those captured in-house under similar culture conditions. **B.** Additional pancreatic cancer cell lines, AsPC-1, MIA PaCa-2, Panc 04 03, T3M4.

Figure 3A shows high-resolution microscope images of three cell lines, BxPC-3, Capan-1, and PANC-1, obtained from our laboratory, alongside corresponding reference images from the American Type Culture Collection (ATCC) database. The visual similarity between the lab's images and those from ATCC confirms the authenticity of the cell lines we are working with. In particular, the consistent cellular morphology, such as the epithelial-like appearance and adherent growth patterns, across both sets of images affirmed that the cells maintained their expected phenotypes during culture, further validating the reliability of our experimental models. In Figure 3B, the morphological assessment is expanded to include additional pancreatic cancer cell lines for which ATCC reference images were not available. These cell lines, similar to the previous set, also exhibited adherent growth patterns typical of epithelial cells. However, despite this common feature, distinct variations in cell shape, size, and arrangement were observed between the different lines, reflecting inherent diversity in their growth characteristics.

Impact of KRAS knockout on cell growth

To assess the impact of KRAS loss on cell growth, small guide RNA (sgRNA) was utilized to knock out KRAS in pancreatic cancer cell lines, followed by an evaluation of

cell viability using the CellTiter-Glo® assay. This luminescence-based assay measures the amount of ATP present, serving as an indirect indicator of cell viability, since ATP levels correlate with metabolically active cells.

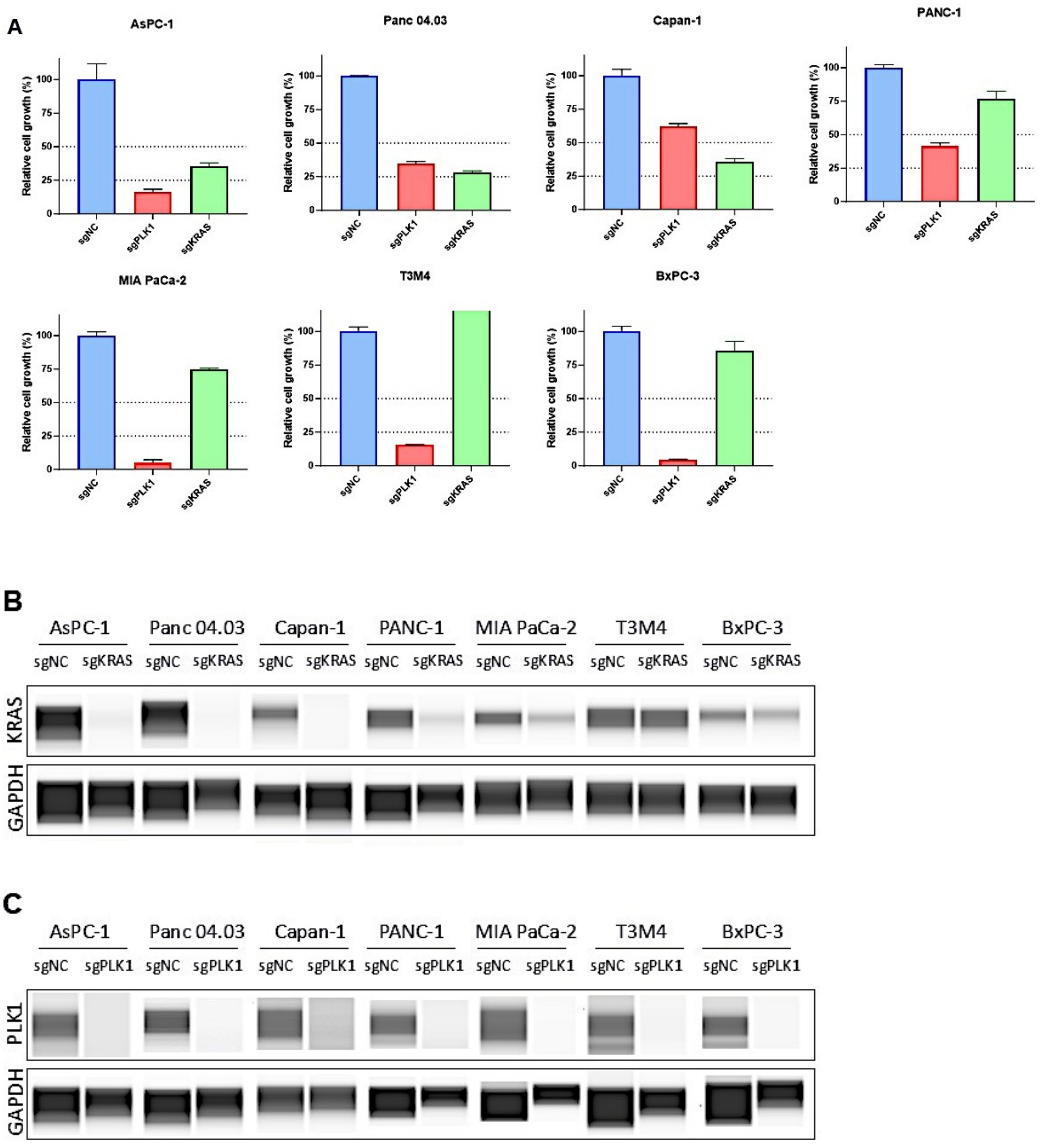

Figure 4. Impact of KRAS knockout on cancer cell growth assessed by CellTiter-Glo® assay. **A.** PLK1 KO was a positive control to confirm the assay conditions. Cells were subjected to KRAS/PLK1 KO using CRISPR/Cas9. Following KO, cells were incubated for 120 hours and then treated with the CellTiter-Glo® reagent to measure ATP levels as an indicator of viable cell number. **B and C.** Confirmation of the KRAS KO using the Jess system. KRAS (B.) and PLK1 (C.) protein expression was measured in cells with KRAS/PLK1 KO compared to controls. Cells were lysed, and protein extracts were analyzed using the Jess system, which allowed for quantitative detection of proteins.

Upon KRAS knockout, a substantial reduction in cell viability was observed in AsPC-1, Panc 04.03, and Capan-1 cells (Figure 4A), underscoring the critical role of KRAS in promoting the growth and survival of these pancreatic cancer cells. This pronounced decrease in viability indicated that loss of KRAS function significantly impaired cellular proliferation, reinforcing its importance as a key oncogenic driver in pancreatic cancer.

To validate the robustness of these findings, a positive control was incorporated by knocking out PLK1, a well-characterized essential gene involved in cell division and widely recognized as critical across multiple cancer types. As expected, PLK1 knockout led to a marked decrease in cell viability, serving as a reliable benchmark for comparison with the KRAS knockout results.

Additionally, knockout efficiency was confirmed at the protein level using the Jess system, an automated capillary-based immunoassay (Figures 4B and 4C). This analysis verified successful depletion of KRAS and PLK1 proteins under the respective experimental conditions, supporting the validity of the observed effects on cell viability.

As noted, KRAS knockout was partial in PANC-1 and MIA PaCa-2 cells, and minimal in T3M4 and BxPC-3. This variability in knockout efficiency likely accounted for the attenuated impact on cell growth observed in these cell lines.

In the T3M4 cell line, an increase in cell number was observed in the sgKRAS-treated cells compared to sgNC controls (118% vs. 100%) (Figure 4A). This apparent increase in growth may be attributed to experimental variation or potential off-target effects, particularly since no KRAS protein depletion was detected in these cells (Figure 4B). The lack of effective KRAS knockout suggested that the observed difference was unlikely to reflect a true biological effect of KRAS loss.

Literature overview of KRAS mutations, expression patterns, and therapeutic potential of targeting KRAS in cancers.

Figure 5A illustrates a word cloud visualized significance of KRAS mutations across a spectrum of cancer types. The relative size of each word correlates with both the frequency of the mutation and its clinical importance, emphasizing mutations that are most associated with malignancies. This visualization underscores the prominence of specific mutations as recurrent drivers across multiple cancer types, including pancreatic cancers. Figure 5B displays a Kaplan-Meier survival analysis (plot from The Human Protein Atlas), which compares the overall survival of pancreatic cancer patients stratified by KRAS expression levels. Patients with high KRAS expressions exhibit significantly poorer survival outcomes compared to those with low KRAS expressions, as indicated by the sharp decline in survival over time for the former. The x-axis represents the survival time in years, while the y-axis denotes the proportion of surviving patients. This finding confirms the unfavorable prognostic role of elevated KRAS

expression in pancreatic cancer, suggesting that high KRAS levels may contribute to more aggressive disease progression and worse clinical outcomes. Figure 5C highlights KRAS protein expression through immunohistochemical (IHC) staining in five representative cancer tissue samples. The samples demonstrate variable KRAS expression across different tumor types, with certain tissues showing strong staining and others exhibiting minimal or no KRAS expression. This heterogeneity underscores the complexity of KRAS dysregulation in cancer and suggests that KRAS expression levels may vary widely depending on the cancer type. Figure 5D provides a comprehensive summary of KRAS protein expression patterns across various cancer types, revealing that moderate to strong immunoreactivity is predominantly observed in cancers such as colorectal, head and neck, stomach, and pancreatic cancers. In contrast, other cancer types, including certain lung and breast cancers, display weak or absent KRAS staining. This variability in KRAS protein expression further supports the notion that KRAS is differentially regulated across malignancies and may have context-dependent roles in tumorigenesis. Figure 5E summarizes the KRAS knockout phenotype data derived from the Mouse Genome Informatics (MGI) database. This data offers critical insights into the biological effects of KRAS deletion in mouse models, highlighting phenotypic consequences that may inform future studies on the functional roles of KRAS in cancer development and progression.

Figure 5F demonstrates the impact of KRAS G12C inhibitors on cell growth inhibition in the MIA PaCa-2 pancreatic cancer cell line. Cells were treated with varying concentrations of KRAS G12C inhibitors over a 120-hour period, and cell viability was assessed using the CellTiter-Glo® assay. The results show a dose-dependent reduction in cell viability, confirming the therapeutic potential of these inhibitors in targeting KRAS-driven cancer cells. This finding is particularly relevant as KRAS G12C mutations have been identified as promising targets for novel cancer therapies. Figure 5G depicts the chemical structures of three KRAS G12C inhibitors: GDC-6036, RMC-6291, and AMG-510. These structures reveal the diversity in the chemical composition of these inhibitors, which are designed to selectively target the mutant KRAS protein. Figure 5H provides an overview of the various KRAS G12C inhibitors currently in development, including their generic names, brand names, and stages of clinical development. This panel emphasizes the progress being made in the development of KRAS-targeted therapies, which hold significant promise for improving treatment outcomes in patients with KRAS-driven cancers.

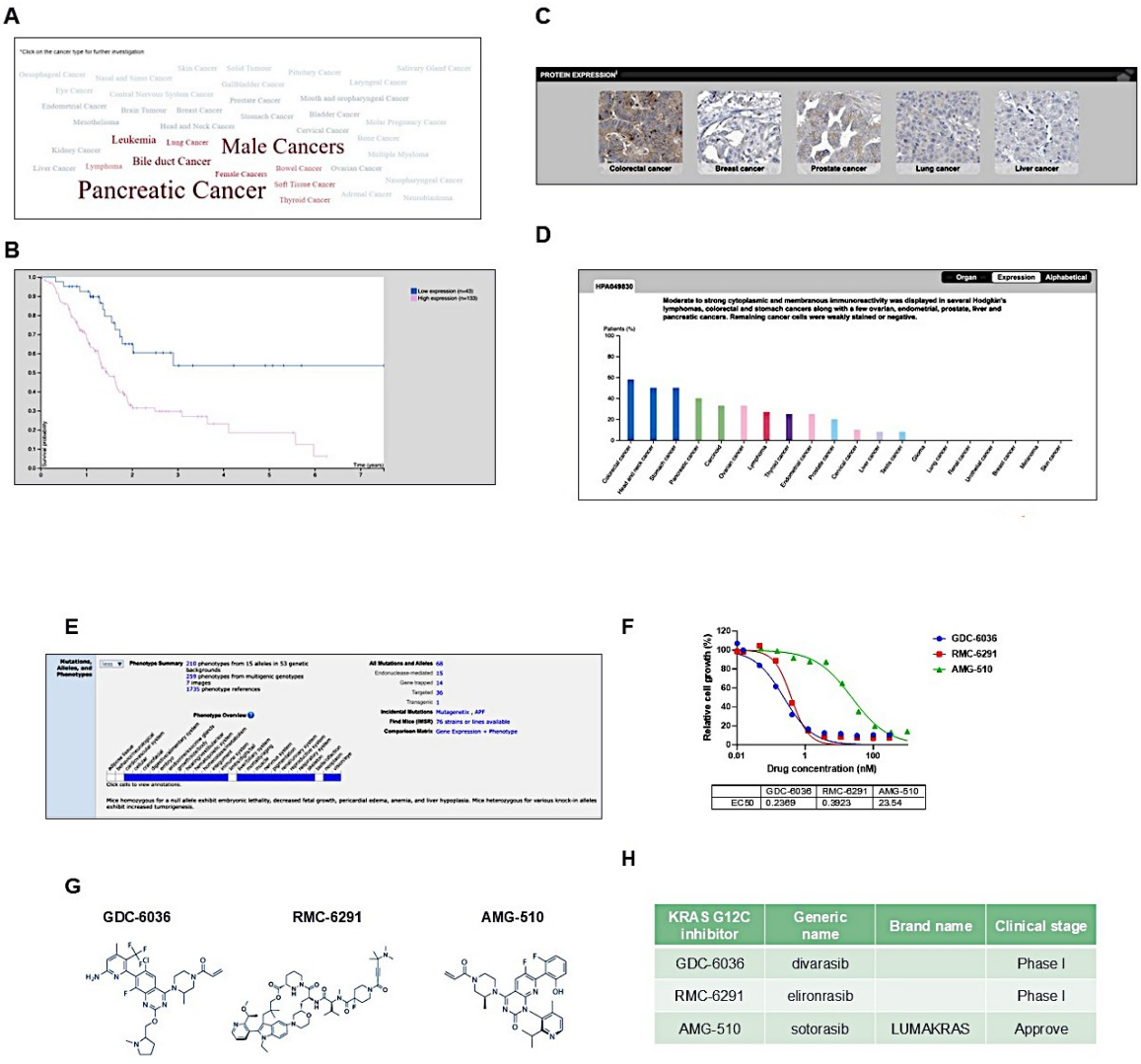

KRAS G12C inhibitor	Generic name	Brand name	Clinical stage
GDC-6036	divarasib		Phase I
RMC-6291	elironrasib		Phase I
AMG-510	sotorasib	LUMAKRAS	Approve

Figure 5. Overview of KRAS mutations, expression patterns, and the therapeutic potential of targeting KRAS in cancers. **A.** Word Cloud visualization of KRAS mutations across different cancer types. The size of each word correlates with the frequency and significance of the mutation within the dataset. **B.** The Kaplan-Meier survival curve compares the overall survival of pancreatic cancer patients with high versus low KRAS expression levels. The x-axis represents the time (years) and the y-axis indicates the proportion of surviving patients. KRAS is prognostic and its high level expression is unfavorable in pancreatic cancer. **C.** KRAS antibody staining in five cancer tissue samples representative of the overall staining pattern. **D.** Summary of KRAS protein expression in cancer tissues. Moderate to strong immunoreactivity was displayed in colorectal, head and neck, stomach, and pancreatic cancers. **E.** Summary of KRAS KO phenotype in the MGI (Mouse Genome Informatics) database. **F.** Cell growth inhibition of MIA PaCa-2 cell line by KRAS G12C inhibitors. Cells were treated with varying concentrations of KRAS inhibitors over a period of 120 hours. Cell viability was measured using the CellTiter-Glo® assay. **G.** The chemical structure of the KRAS G12C inhibitors. H. Overview of various KRAS G12C inhibitors, listing their generic names, brand names, and current clinical development stages.

Discussion

The results of this study underscore the critical role of KRAS as a selective target for pancreatic cancer. Through the DepMap analysis, it became evident that KRAS is not merely an essential oncogene in a broad range of cancers but exhibited a specific dependency in tumor types where KRAS mutations are most prevalent, such as pancreatic, colorectal, and lung cancers (Figure 1). This tumor-type-specific KRAS dependency aligned with the known biology of KRAS, reinforcing its context-dependent role as an oncogenic driver. The comparison between KRAS and other essential genes like PLK1 further emphasized that KRAS represented a selective vulnerability in certain cancers, offering an attractive therapeutic target, especially in the case of pancreatic cancer where alternative treatment options remain scarce.

Consistent with the above observations, both CRISPR knockout and RNAi screens demonstrated that cancer cells harboring KRAS mutations showed a significant reliance on the continuous activity of KRAS for survival. The consistency of KRAS dependency across multiple methodologies (CRISPR and RNAi) added robust validation to the findings and underscored the oncogene's indispensable role in cancer cell viability (Figure 2)

Moreover, the morphological analysis of these pancreatic cancer cell lines confirmed their epithelial-like phenotype and growth characteristics, lending further support to the validity of the experimental models used in this work (Figure 3). Despite their shared epithelial morphology, the differences observed between the cell lines in terms of cell shape, size, and arrangement reflect the inherent heterogeneity of pancreatic cancer and suggest that KRAS-targeted therapies may need to account for this variability when applied clinically. These morphological variations could also serve as indicators of different KRAS-driven oncogenic pathways or resistance mechanisms, which warrant further investigation.

The impact of KRAS knockout on pancreatic cancer cell growth, as demonstrated by the viability assays, reaffirmed the pivotal role of KRAS in maintaining tumor cell survival (Figure 4). Furthermore, the concurrent validation of PLK1 as a positive control confirmed that the experimental system was robust and the observed effects were specific to KRAS loss. The verification of knockout efficiency at the protein level through the Jess system further strengthened the reliability of these results (Figures 4B and 4C), solidifying the rationale for continued development of KRAS inhibitors in KRAS-driven cancers.

Literature suggests that cancer cells with mutant Ras, experience elevated mitotic stress and are more dependent on key mitotic regulators such as PLK1 (14). However, in this study, the complete knockout of PLK1 in KRAS-mutant pancreatic cancer cell lines alongside KRAS wild-type line (BxPC-3) resulted in significant cell growth inhibition. These findings indicate that the impact of PLK1 loss is robust across genotypes and supports its role as a broadly essential gene. Reciprocal protein depletion was not assessed

between KRAS and PLK1 knockouts, and to our knowledge, no direct regulatory relationship between these proteins has been established.

A detailed literature exploration of KRAS mutations and expression patterns across various cancer types revealed that KRAS mutations were recurrent drivers in multiple malignancies (Figure 5A). Elevated KRAS expression, especially in pancreatic cancer, was associated with poorer survival outcomes, confirming the oncogene's unfavorable prognostic significance (Figure 5B). The variability of KRAS expressions across different cancer types, as demonstrated through immunohistochemical staining, further emphasized that KRAS dysregulation was highly context-dependent, with certain cancers displaying strong KRAS expression while others showing weak or no expression (Figures 5C and 5D). These data suggested that KRAS-targeted therapies may need to be tailored to tumor-specific contexts, with careful consideration of KRAS expression levels and mutation status.

The literature search also confirmed the efficacy of KRAS G12C inhibitors in reducing the viability of pancreatic cancer cells harboring KRAS mutations (Figure 5F). This observation is particularly relevant given the longstanding challenge of targeting KRAS, which was once considered "undruggable." The dose-dependent inhibition of cell growth following treatment with KRAS G12C inhibitors underscores their potential as viable therapeutic agents, especially in cancers where KRAS G12C mutations are prevalent. The chemical structures of these inhibitors (Figure 5G) and their current stages of clinical development (Figure 5H) provide further evidence of the progress being made in the development of KRAS-targeted therapies, offering renewed hope for patients with KRAS-driven cancers.

Conclusion

This study reinforced the concept of KRAS as a selective and context-dependent therapeutic target, particularly in pancreatic cancer where alternative treatment options are limited. The results not only highlighted the importance of targeting KRAS mutations but also emphasized the need for personalized approaches to treatment, given the variability in KRAS dependency and expression across different cancer types. Future research should focus on overcoming resistance mechanisms to KRAS inhibitors and expanding the range of druggable KRAS mutations. As KRAS inhibitors advance through clinical development, they hold great promise for improving treatment outcomes in patients with KRAS-driven malignancies, potentially transforming the landscape of cancer therapy.

Acknowledgements

I would like to sincerely thank Dr. Chiou-Hong Lin for her invaluable mentorship and support throughout the course of this work. Special thanks to John Vu and Mint Sirisawad for their expert guidance in experimental design and execution. I am also deeply grateful for the opportunity to contribute to research efforts at Scorpion Therapeutics, which provided a rich

and rewarding environment for scientific growth.

References

1. Tsherniak, A., Vazquez, F., Montgomery, P. G., Weir, B. A., Kryukov, G., Cowley, G. S., et al. (2017). Defining a cancer dependency map. Cell, 170: 564-576. https://pubmed.ncbi.nlm.nih.gov/28753430/

2. Drosten, M., Barbacid, M. (2020). Targeting the MAPK Pathway in KRAS-Driven Tumors. Cancer Cell, 37: 543-550. https://pubmed.ncbi.nlm.nih.gov/32289276/

3. Luo, J. (2021). KRAS mutation in pancreatic cancer. Semin. Oncol., 48: 10-18. https://pubmed.ncbi.nlm.nih.gov/33676749/

4. Yang, Y., Zhang, H., Huang, S., Chu, Q. (2023). KRAS mutations in solid tumors: characteristics, current therapeutic strategy, and potential treatment exploration. J. Clin. Med., 12: 709-732. https://pubmed.ncbi.nlm.nih.gov/36675641/

5. Ferreira, A., Pereira, F., Reis, C., Oliveira, M. J., Sousa, M. J., Preto, A. (2022). Crucial role of oncogenic KRAS mutations in apoptosis and autophagy regulation: therapeutic implications. Cells, 11: 2183-2205. https://pubmed.ncbi.nlm.nih.gov/35883626/

6. Salgia, R., Pharaon, R., Mambetsariev, I., Nam, A., Sattler, M. (2021). The improbable targeted therapy: KRAS as an emerging target in non-small cell lung cancer (NSCLC). Cell Rep. Med., 2: 100186-100200. https://pubmed.ncbi.nlm.nih.gov/33521700/

7. Bansal, I., Pandey, A. K., Ruwali, M. (2023). Small-molecule inhibitors of kinases in breast cancer therapy: recent advances, opportunities, and challenges. Front. Pharmacol., 14: 1244597-1244608. https://pubmed.ncbi.nlm.nih.gov/37711177/

8. Ma, Y. S., Xin, R., Yang, X. L., Shi, Y., Zhang, D. D., Wang, H. M., et al. (2021). Paving the way for small-molecule drug discovery. Am. J. Transl. Res., 13: 853-870. https://pubmed.ncbi.nlm.nih.gov/33841626/

9. Chang, W. H., Nguye,n T. T., Hsu, C. H., Bryant, K. L., Kim, H. J., Ying, H., et al. (2021). KRAS-dependent cancer cells promote survival by producing exosomes enriched in Survivin. Cancer Lett., 517: 66-77. https://pubmed.ncbi.nlm.nih.gov/34111513/

10. Padilla, J., Lee, B. S., Kim, A., Park, Y. I., Bansal, A., Lee, J. (2025). Tumor regulatory effect of 15-hydroxyprostaglandin dehydrogenase (HPGD) in triple-negative breast cancer. Int. J. Mol. Sci., 26: 1912- 1926. https://pubmed.ncbi.nlm.nih.gov/40076539/

11. Sormunen, A., Koivulehto, E., Alitalo, K., Saksela, K., Laham-Karam, N., Ylä-Herttuala, S. (2023). Comparison of automated and traditional western blotting methods. Methods Protoc., 6: 43-52. https://pubmed.ncbi.nlm.nih.gov/37104025/

12. Mahadevan, K. K., McAndrews, K. M., LeBleu, V. S., Yang, S., Lyu, H., Li, B., et al. (2023). $KRAS^{G12D}$ inhibition reprograms the microenvironment of early and advanced pancreatic cancer to promote FAS-mediated killing by $CD8^{+}$ T cells. Cancer Cell, 41: 1606-1620. https://pubmed.ncbi.nlm.nih.gov/37625401/

13. Seki, A., Rutz, S. (2018). Optimized RNP transfection for highly efficient CRISPR/Cas9-mediated gene knockout in primary T cells. J. Exp. Med., 215: 985-997. https://pubmed.ncbi.nlm.nih.gov/29436394/

14. Luo, J., Emanuele, M. J., Li, D., Creighton, C. J., Schlabach, M. R., Westbrook, T. F., et al. (2009). A genome-wide RNAi screen identifies multiple synthetic lethal interactions with the Ras oncogene. Cell, 137: 835-848. https://pubmed.ncbi.nlm.nih.gov/19490893/